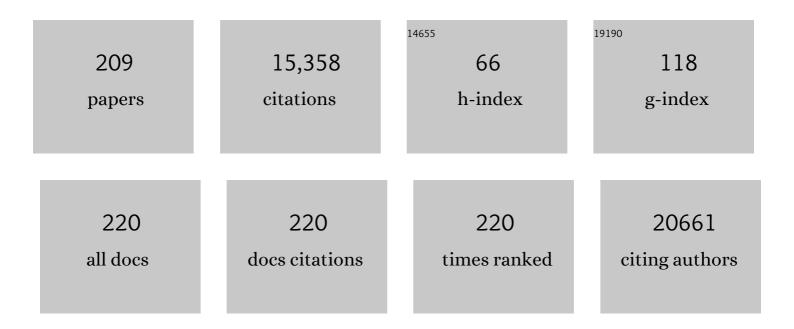
Ki Tae Nam

List of Publications by Year in descending order

Source: https://exaly.com/author-pdf/647779/publications.pdf Version: 2024-02-01



KI TAF NAM

#	Article	IF	CITATIONS
1	Highâ€Throughput Pb Recycling for Perovskite Solar Cells Using Biomimetic Whitlockite. Energy and Environmental Materials, 2023, 6, .	12.8	8
2	Electronic interaction between transition metal single-atoms and anatase TiO ₂ boosts CO ₂ photoreduction with H ₂ O. Energy and Environmental Science, 2022, 15, 601-609.	30.8	88
3	Random Lasing with a High Degree of Circular Dichroism by Chiral Plasmonic Gold Nanoparticles. ACS Photonics, 2022, 9, 613-620.	6.6	9
4	Ultrasensitive Nearâ€Infrared Circularly Polarized Light Detection Using 3D Perovskite Embedded with Chiral Plasmonic Nanoparticles. Advanced Science, 2022, 9, e2104598.	11.2	23
5	A Sn doped, strained CuAg film for electrochemical CO ₂ reduction. Journal of Materials Chemistry A, 2022, 10, 7082-7089.	10.3	6
6	Fabrication of Ni–Mo-based Electrocatalysts by Modified Zn Phosphating for Hydrogen Evolution Reaction. Journal of Electrochemical Science and Technology, 2022, 13, 54-62.	2.2	1
7	Second Harmonic Optical Circular Dichroism of Plasmonic Chiral Helicoid-III Nanoparticles. ACS Photonics, 2022, 9, 784-792.	6.6	16
8	Humidity-induced synaptic plasticity of ZnO artificial synapses using peptide insulator for neuromorphic computing. Journal of Materials Science and Technology, 2022, 119, 150-155.	10.7	11
9	Adenine oligomer directed synthesis of chiral gold nanoparticles. Nature Communications, 2022, 13, .	12.8	31
10	Tyrosyltyrosylcysteine-Directed Synthesis of Chiral Cobalt Oxide Nanoparticles and Peptide Conformation Analysis. ACS Nano, 2021, 15, 979-988.	14.6	19
11	Capturing Manganese Oxide Intermediates in Electrochemical Water Oxidation at Neutral pH by In Situ Raman Spectroscopy. Angewandte Chemie, 2021, 133, 4723-4731.	2.0	5
12	Capturing Manganese Oxide Intermediates in Electrochemical Water Oxidation at Neutral pH by In Situ Raman Spectroscopy. Angewandte Chemie - International Edition, 2021, 60, 4673-4681.	13.8	41
13	Engineered Dissolution for Better Electrocatalysts. CheM, 2021, 7, 20-22.	11.7	0
14	Revealing Structural Disorder in Hydrogenated Amorphous Silicon for a Low‣oss Photonic Platform at Visible Frequencies. Advanced Materials, 2021, 33, e2005893.	21.0	69
15	Effects of paramagnetic fluctuations on the thermochemistry of MnO(100) surfaces in the oxygen evolution reaction. Physical Chemistry Chemical Physics, 2021, 23, 859-865.	2.8	4
16	Gold meets peptides in a hybrid coil. Science, 2021, 371, 1311-1311.	12.6	4
17	Dimensionality reduction and unsupervised clustering for EELS-SI. Ultramicroscopy, 2021, 231, 113314.	1.9	9
18	Synergistic Effects of Nonmagnetic Carbon Nanotubes on the Performance and Stability of Magnetorheological Fluids Containing Carbon Nanotube-Co _{0.4} Fe _{0.4} Ni _{0.2} Nanocomposite Particles. Nano Letters, 2021, 21, 4973-4980.	9.1	12

#	Article	IF	CITATIONS
19	In Situ Growth of CoMnPOxHy for Oxygen Evolution Reaction by Cobalt-Modified Commercial Manganese Phosphating and Electrochemical Activation. ACS Applied Energy Materials, 2021, 4, 5392-5396.	5.1	1
20	Fully Degradable Memristors and Humidity Sensors Based on a Tyrosine-Rich Peptide. ACS Applied Electronic Materials, 2021, 3, 3372-3378.	4.3	14
21	Complex Impedance Analysis on Charge Accumulation Step of Mn ₃ O ₄ Nanoparticles during Water Oxidation. ACS Omega, 2021, 6, 18404-18413.	3.5	5
22	Redox-neutral electrochemical conversion of CO2 to dimethyl carbonate. Nature Energy, 2021, 6, 733-741.	39.5	55
23	Electrochemical Synthesis of Glycine from Oxalic Acid and Nitrate. Angewandte Chemie, 2021, 133, 22114-22122.	2.0	4
24	Electrochemical Synthesis of Glycine from Oxalic Acid and Nitrate. Angewandte Chemie - International Edition, 2021, 60, 21943-21951.	13.8	55
25	Metal Halide Perovskites for Solar Fuel Production and Photoreactions. Journal of Physical Chemistry Letters, 2021, 12, 8292-8301.	4.6	17
26	Inorganic Hollow Nanocoils Fabricated by Controlled Interfacial Reaction and Their Electrocatalytic Properties. Small, 2021, 17, e2103575.	10.0	1
27	Electrochemically Activated NiFeO _{<i>x</i>} H _{<i>y</i>} for Enhanced Oxygen Evolution. ACS Applied Energy Materials, 2021, 4, 595-601.	5.1	10
28	Electrolysis of iron with oxygen gas evolution from molten sodium borate electrolytes. Ironmaking and Steelmaking, 2021, 48, 1030-1037.	2.1	4
29	Controlling the size and circular dichroism of chiral gold helicoids. Materials Advances, 2021, 2, 6988-6995.	5.4	20
30	Synaptic transistors based on a tyrosine-rich peptide for neuromorphic computing. RSC Advances, 2021, 11, 39619-39624.	3.6	2
31	Recent advances in heterogeneous Mn-based electrocatalysts toward biological photosynthetic Mn4Ca cluster. Catalysis Today, 2020, 353, 232-241.	4.4	9
32	Light polarization dependency existing in the biological photosystem and possible implications for artificial antenna systems. Photosynthesis Research, 2020, 143, 205-220.	2.9	2
33	Chiral 432 Helicoid II Nanoparticle Synthesized with Glutathione and Poly(T) ₂₀ Nucleotide. ChemNanoMat, 2020, 6, 362-367.	2.8	20
34	Plasmonic metamaterials for chiral sensing applications. Nanoscale, 2020, 12, 58-66.	5.6	98
35	Importance of Interfacial Band Structure between the Substrate and Mn ₃ O ₄ Nanocatalysts during Electrochemical Water Oxidation. ACS Catalysis, 2020, 10, 1237-1245.	11.2	23
36	Electrochemical β‣elective Hydrocarboxylation of Styrene Using CO ₂ and Water. Advanced Science, 2020, 7, 1900137.	11.2	38

Ki Tae Nam

#	Article	IF	CITATIONS
37	Chiral Surface and Geometry of Metal Nanocrystals. Advanced Materials, 2020, 32, e1905758.	21.0	85
38	Chemically Deposited Amorphous Zn-Doped NiFeO <i>_{<i>x</i>}</i> H <i>_{<i>y</i>}</i> for Enhanced Water Oxidation. ACS Catalysis, 2020, 10, 235-244.	11.2	86
39	Metal Nanocrystals: Chiral Surface and Geometry of Metal Nanocrystals (Adv. Mater. 41/2020). Advanced Materials, 2020, 32, 2070308.	21.0	0
40	Electrochemical C–N Bond Formation for Sustainable Amine Synthesis. Trends in Chemistry, 2020, 2, 1004-1019.	8.5	56
41	Spectroscopic capture of a low-spin Mn(IV)-oxo species in Ni–Mn3O4 nanoparticles during water oxidation catalysis. Nature Communications, 2020, 11, 5230.	12.8	21
42	Proton-enabled activation of peptide materials for biological bimodal memory. Nature Communications, 2020, 11, 5896.	12.8	36
43	Hierarchically Structured Fe ₃ O ₄ Nanoparticles for High-Performance Magnetorheological Fluids with Long-Term Stability. ACS Applied Nano Materials, 2020, 3, 10931-10940.	5.0	21
44	Tyrosineâ€Rich Peptide Insulator for Rapidly Dissolving Transient Electronics. Advanced Materials Technologies, 2020, 5, 2000516.	5.8	7
45	A Single Chiral Nanoparticle Induced Valley Polarization Enhancement. Small, 2020, 16, e2003005.	10.0	18
46	An Implantable Ionic Wireless Power Transfer System Facilitating Electrosynthesis. ACS Nano, 2020, 14, 11743-11752.	14.6	10
47	Vitamin B12â€Immobilized Graphene Oxide for Efficient Electrocatalytic Carbon Dioxide Reduction Reaction. ChemSusChem, 2020, 13, 5620-5624.	6.8	10
48	Valley Polarization: A Single Chiral Nanoparticle Induced Valley Polarization Enhancement (Small) Tj ETQq0 0 0 r	gBT /Overl	ock 10 Tf 50 3
49	γâ€Glutamylcysteine―and Cysteinylglycineâ€Directed Growth of Chiral Gold Nanoparticles and their Crystallographic Analysis. Angewandte Chemie, 2020, 132, 13076-13083.	2.0	7
50	Chirality control of inorganic materials and metals by peptides or amino acids. Materials Advances, 2020, 1, 512-524.	5.4	29
51	A scalable Al–Ni alloy powder catalyst prepared by metallurgical microstructure control. Journal of Materials Chemistry A, 2020, 8, 11133-11140.	10.3	6
52	Manganese oxide-based heterogeneous electrocatalysts for water oxidation. Energy and Environmental Science, 2020, 13, 2310-2340.	30.8	81
53	Electrocatalytic Reduction of CO ₂ to Ethylene by Molecular Cuâ€Complex Immobilized on Graphitized Mesoporous Carbon. Small, 2020, 16, e2000955.	10.0	48
54	Single Nanoparticle Chiroptics in a Liquid: Optical Activity in Hyper-Rayleigh Scattering from Au Helicoids. Nano Letters, 2020, 20, 5792-5798.	9.1	32

#	Article	IF	CITATIONS
55	Probing the Structure and Binding Mode of EDTA on the Surface of Mn ₃ O ₄ Nanoparticles for Water Oxidation by Advanced Electron Paramagnetic Resonance Spectroscopy. Inorganic Chemistry, 2020, 59, 8846-8854.	4.0	2
56	Quantitative analysis of the coupling between proton and electron transport in peptide/manganese oxide hybrid films. Physical Chemistry Chemical Physics, 2020, 22, 7537-7545.	2.8	8
57	Uniform Chiral Gap Synthesis for High Dissymmetry Factor in Single Plasmonic Gold Nanoparticle. ACS Nano, 2020, 14, 3595-3602.	14.6	84
58	Electrochemical cell in the brain. Nature Nanotechnology, 2020, 15, 625-626.	31.5	2
59	Cysteine-encoded chirality evolution in plasmonic rhombic dodecahedral gold nanoparticles. Nature Communications, 2020, 11, 263.	12.8	145
60	Redox-Active Tyrosine-Mediated Peptide Template for Large-Scale Single-Crystalline Two-Dimensional Silver Nanosheets. ACS Nano, 2020, 14, 1738-1744.	14.6	16
61	Nickelâ€Ðoping Effect on Mn ₃ O ₄ Nanoparticles for Electrochemical Water Oxidation under Neutral Condition. Small Methods, 2020, 4, 1900733.	8.6	36
62	Uniform, Assembled 4 nm Mn ₃ O ₄ Nanoparticles as Efficient Water Oxidation Electrocatalysts at Neutral pH. Advanced Functional Materials, 2020, 30, 1910424.	14.9	55
63	Mechanistic Investigation of Biomass Oxidation Using Nickel Oxide Nanoparticles in a CO ₂ -Saturated Electrolyte for Paired Electrolysis. Journal of Physical Chemistry Letters, 2020, 11, 2941-2948.	4.6	88
64	γâ€Glutamylcysteine―and Cysteinylglycineâ€Directed Growth of Chiral Gold Nanoparticles and their Crystallographic Analysis. Angewandte Chemie - International Edition, 2020, 59, 12976-12983.	13.8	59
65	Kerker onditioned Dynamic Cryptographic Nanoprints. Advanced Optical Materials, 2019, 7, 1801070.	7.3	50
66	Chiral Scatterometry on Chemically Synthesized Single Plasmonic Nanoparticles. ACS Nano, 2019, 13, 8659-8668.	14.6	69
67	Defect-engineered MoS ₂ with extended photoluminescence lifetime for high-performance hydrogen evolution. Journal of Materials Chemistry C, 2019, 7, 10173-10178.	5.5	34
68	Importance of Entropic Contribution to Electrochemical Water Oxidation Catalysis. ACS Energy Letters, 2019, 4, 1918-1929.	17.4	31
69	Wavelength-decoupled geometric metasurfaces by arbitrary dispersion control. Communications Physics, 2019, 2, .	5.3	44
70	Anion Extraction-Induced Polymorph Control of Transition Metal Dichalcogenides. Nano Letters, 2019, 19, 8644-8652.	9.1	12
71	Cyclic two-step electrolysis for stable electrochemical conversion of carbon dioxide to formate. Nature Communications, 2019, 10, 3919.	12.8	76
72	Bioinspired Toolkit Based on Intermolecular Encoder toward Evolutionary 4D Chiral Plasmonic Materials. Accounts of Chemical Research, 2019, 52, 2768-2783.	15.6	41

#	Article	IF	CITATIONS
73	Methylamine Treated Mn3O4Nanoparticles as a Highly Efficient Water Oxidation Catalyst under Neutral Condition. ChemCatChem, 2019, 11, 1665-1672.	3.7	14
74	Mechanistic Investigation with Kinetic Parameters on Water Oxidation Catalyzed by Manganese Oxide Nanoparticle Film. ACS Sustainable Chemistry and Engineering, 2019, 7, 10595-10604.	6.7	28
75	Reversible and cooperative photoactivation of single-atom Cu/TiO2 photocatalysts. Nature Materials, 2019, 18, 620-626.	27.5	501
76	Size-controllable and uniform gold bumpy nanocubes for single-particle-level surface-enhanced Raman scattering sensitivity. Physical Chemistry Chemical Physics, 2019, 21, 9044-9051.	2.8	10
77	Cysteine Induced Chiral Morphology in Palladium Nanoparticle. Particle and Particle Systems Characterization, 2019, 36, 1900062.	2.3	29
78	Achieving highly efficient CO ₂ to CO electroreduction exceeding 300 mA cm ^{â^'2} with single-atom nickel electrocatalysts. Journal of Materials Chemistry A, 2019, 7, 10651-10661.	10.3	165
79	Tunable Metasurfaces: Kerkerâ€Conditioned Dynamic Cryptographic Nanoprints (Advanced Optical) Tj ETQq1 1	0.784314 7.3	rgBT /Overic
80	DNA translocation through a nanopore in an ultrathin self-assembled peptide membrane. Nanotechnology, 2019, 30, 195602.	2.6	2
81	Highly Selective Active Chlorine Generation Electrocatalyzed by Co ₃ O ₄ Nanoparticles: Mechanistic Investigation through in Situ Electrokinetic and Spectroscopic Analyses. Journal of Physical Chemistry Letters, 2019, 10, 1226-1233.	4.6	44
82	Demonstration of the nanosize effect of carbon nanomaterials on the dehydrogenation temperature of ammonia borane. Nanoscale Advances, 2019, 1, 4697-4703.	4.6	13
83	Metasurface zone plate for light manipulation in vectorial regime. Communications Physics, 2019, 2, .	5.3	35
84	Tyrosineâ€Rich Peptides as a Platform for Assembly and Material Synthesis. Advanced Science, 2019, 6, 1801255.	11.2	91
85	Hydrogen Production via Water Electrolysis: The Benefits of a Solar Cell-Powered Process. IEEE Electrification Magazine, 2018, 6, 19-25.	1.8	12
86	Identifying peptide sequences that can control the assembly of gold nanostructures. Molecular Systems Design and Engineering, 2018, 3, 581-590.	3.4	25
87	Amino-acid- and peptide-directed synthesis of chiral plasmonic gold nanoparticles. Nature, 2018, 556, 360-365.	27.8	785
88	Tailoring a Tyrosine-Rich Peptide into Size- and Thickness-Controllable Nanofilms. ACS Omega, 2018, 3, 3901-3907.	3.5	17
89	Electrochemical Analysis of Carbon Nanosheet Catalyst on Silicon Photocathode for Hydrogen Generation. Bulletin of the Korean Chemical Society, 2018, 39, 356-362.	1.9	4
90	Defining a Materials Database for the Design of Copper Binary Alloy Catalysts for Electrochemical CO ₂ Conversion. Advanced Materials, 2018, 30, e1704717.	21.0	150

#	Article	IF	CITATIONS
91	Selective Electrochemical Production of Formate from Carbon Dioxide with Bismuth-Based Catalysts in an Aqueous Electrolyte. ACS Catalysis, 2018, 8, 931-937.	11.2	190
92	Pragmatic Metasurface Hologram at Visible Wavelength: The Balance between Diffraction Efficiency and Fabrication Compatibility. ACS Photonics, 2018, 5, 1643-1647.	6.6	87
93	Electrophoretic kinetics of concentrated TiO2 nanoparticle suspensions in aprotic solvent. Electronic Materials Letters, 2018, 14, 79-82.	2.2	2
94	Effects of proton conduction on dielectric properties of peptides. RSC Advances, 2018, 8, 34047-34055.	3.6	9
95	Frontispiece: Tris(2â€benzimidazolylmethyl)amineâ€Directed Synthesis of Singleâ€Atom Nickel Catalysts for Electrochemical CO Production from CO 2. Chemistry - A European Journal, 2018, 24, .	3.3	0
96	Involvement of high-valent manganese-oxo intermediates in oxidation reactions: realisation in nature, nano and molecular systems. Nano Convergence, 2018, 5, 18.	12.1	30
97	Recent advances and perspectives of halide perovskite photocatalyst. Current Opinion in Electrochemistry, 2018, 11, 98-104.	4.8	24
98	Historical Perspectives of the Development of Materials Science and Engineering Program at Seoul National University and Vision. Advanced Materials, 2018, 30, 1804800.	21.0	0
99	Solar Water Splitting: Efficient Water Splitting Cascade Photoanodes with Ligand-Engineered MnO Cocatalysts (Adv. Sci. 10/2018). Advanced Science, 2018, 5, 1870061.	11.2	0
100	Physically Transient Field-Effect Transistors Based on Black Phosphorus. ACS Applied Materials & Interfaces, 2018, 10, 42630-42636.	8.0	22
101	Outfitting Next Generation Displays with Optical Metasurfaces. ACS Photonics, 2018, 5, 3876-3895.	6.6	118
102	Quantitative Analysis of Calcium Phosphate Nanocluster Growth Using Time-of-Flight Medium-Energy-Ion-Scattering Spectroscopy. ACS Central Science, 2018, 4, 1253-1260.	11.3	5
103	Hierarchical carbon–silicon nanowire heterostructures for the hydrogen evolution reaction. Nanoscale, 2018, 10, 13936-13941.	5.6	20
104	Synthetic Mechanism Discovery of Monophase Cuprous Oxide for Record High Photoelectrochemical Conversion of CO ₂ to Methanol in Water. ACS Nano, 2018, 12, 8187-8196.	14.6	44
105	Active Color Control in a Metasurface by Polarization Rotation. Applied Sciences (Switzerland), 2018, 8, 982.	2.5	42
106	Geometric metasurface enabling polarization independent beam splitting. Scientific Reports, 2018, 8, 9468.	3.3	53
107	New challenges of electrokinetic studies in investigating the reaction mechanism of electrochemical CO ₂ reduction. Journal of Materials Chemistry A, 2018, 6, 14043-14057.	10.3	118
108	Efficient Water Splitting Cascade Photoanodes with Ligandâ€Engineered MnO Cocatalysts. Advanced Science, 2018, 5, 1800727.	11.2	30

#	Article	IF	CITATIONS
109	Tris(2â€benzimidazolylmethyl)amineâ€Directed Synthesis of Singleâ€Atom Nickel Catalysts for Electrochemical CO Production from CO ₂ . Chemistry - A European Journal, 2018, 24, 18444-18454.	3.3	50
110	Polydopamine–Copper Hybrid Films as Source and Drain for Oxide Semiconductor Fieldâ€Effect Transistors. Advanced Electronic Materials, 2018, 4, 1800046.	5.1	1
111	"Crypto-Display―in Dual-Mode Metasurfaces by Simultaneous Control of Phase and Spectral Responses. ACS Nano, 2018, 12, 6421-6428.	14.6	130
112	Catalytic synergy effect of MoS ₂ /reduced graphene oxide hybrids for a highly efficient hydrogen evolution reaction. RSC Advances, 2017, 7, 5480-5487.	3.6	67
113	Double-Layer Graphene Outperforming Monolayer as Catalyst on Silicon Photocathode for Hydrogen Production. ACS Applied Materials & Interfaces, 2017, 9, 3570-3580.	8.0	20
114	Current Status and Bioinspired Perspective of Electrochemical Conversion of CO ₂ to a Long-Chain Hydrocarbon. Journal of Physical Chemistry Letters, 2017, 8, 538-545.	4.6	109
115	Controlled Molybdenum Disulfide Assembly inside Carbon Nanofiber by Boudouard Reaction Inspired Selective Carbon Oxidation. Advanced Materials, 2017, 29, 1605327.	21.0	14
116	Sulfur-Modified Graphitic Carbon Nitride Nanostructures as an Efficient Electrocatalyst for Water Oxidation. Small, 2017, 13, 1603893.	10.0	52
117	High-Density Single-Layer Coating of Gold Nanoparticles onto Multiple Substrates by Using an Intrinsically Disordered Protein of α-Synuclein for Nanoapplications. ACS Applied Materials & Interfaces, 2017, 9, 8519-8532.	8.0	8
118	Photocatalytic hydrogen generation from hydriodic acid using methylammonium lead iodide in dynamic equilibrium with aqueous solution. Nature Energy, 2017, 2, .	39.5	438
119	Reaction Mechanisms of the Electrochemical Conversion of Carbon Dioxide to Formic Acid on Tin Oxide Electrodes. ChemElectroChem, 2017, 4, 2130-2136.	3.4	76
120	Plasmon Enhanced Fluorescence Based on Porphyrin–Peptoid Hybridized Gold Nanoparticle Platform. Small, 2017, 13, 1700071.	10.0	21
121	Screening of Pro–Asp Sequences Exposed on Bacteriophage M13 as an Ideal Anchor for Gold Nanocubes. ACS Synthetic Biology, 2017, 6, 1635-1641.	3.8	4
122	Chondroitin Sulfate-Based Biomineralizing Surface Hydrogels for Bone Tissue Engineering. ACS Applied Materials & Interfaces, 2017, 9, 21639-21650.	8.0	118
123	Amorphous Cobalt Phyllosilicate with Layered Crystalline Motifs as Water Oxidation Catalyst. Advanced Materials, 2017, 29, 1606893.	21.0	84
124	Design Principle and Loss Engineering for Photovoltaic–Electrolysis Cell System. ACS Omega, 2017, 2, 1009-1018.	3.5	57
125	Mechanistic Investigation of Water Oxidation Catalyzed by Uniform, Assembled MnO Nanoparticles. Journal of the American Chemical Society, 2017, 139, 2277-2285.	13.7	133
126	p-Type CuBi 2 O 4 thin films prepared by flux-mediated one-pot solution process with improved structural and photoelectrochemical characteristics. Materials Letters, 2017, 188, 192-196.	2.6	34

ΚΙ ΤΑΕ ΝΑΜ

#	Article	IF	CITATIONS
127	Morphologyâ€Directed Selective Production of Ethylene or Ethane from CO ₂ on a Cu Mesopore Electrode. Angewandte Chemie, 2017, 129, 814-818.	2.0	57
128	Morphologyâ€Directed Selective Production of Ethylene or Ethane from CO ₂ on a Cu Mesopore Electrode. Angewandte Chemie - International Edition, 2017, 56, 796-800.	13.8	268
129	Increased electrical conductivity of peptides through annealing process. APL Materials, 2017, 5, .	5.1	9
130	Reverse Electrodialysis-Assisted Solar Water Splitting. Scientific Reports, 2017, 7, 12281.	3.3	7
131	Arginine-Presenting Peptide Hydrogels Decorated with Hydroxyapatite as Biomimetic Scaffolds for Bone Regeneration. Biomacromolecules, 2017, 18, 3541-3550.	5.4	78
132	Dielectric Meta-Holograms Enabled with Dual Magnetic Resonances in Visible Light. ACS Nano, 2017, 11, 9382-9389.	14.6	157
133	Biomoleculeâ€Enabled Chiral Assembly of Plasmonic Nanostructures. ChemNanoMat, 2017, 3, 685-697.	2.8	41
134	Proton Conduction in a Tyrosineâ€Rich Peptide/Manganese Oxide Hybrid Nanofilm. Advanced Functional Materials, 2017, 27, 1702185.	14.9	23
135	Rise of nano effects in electrode during electrocatalytic CO ₂ conversion. Nanotechnology, 2017, 28, 352001.	2.6	19
136	Biomimetic whitlockite inorganic nanoparticles-mediated in situ remodeling and rapid bone regeneration. Biomaterials, 2017, 112, 31-43.	11.4	124
137	Water Oxidation Mechanism for 3d Transition Metal Oxide Catalysts under Neutral Condition. Journal of the Korean Ceramic Society, 2017, 54, 1-8.	2.3	24
138	Highly Active MnO Catalysts Integrated onto Fe ₂ O ₃ Nanorods for Efficient Water Splitting. Advanced Materials Interfaces, 2016, 3, 1600176.	3.7	22
139	A wafer-scale antireflective protection layer of solution-processed TiO ₂ nanorods for high performance silicon-based water splitting photocathodes. Journal of Materials Chemistry A, 2016, 4, 9477-9485.	10.3	47
140	Theoretical and Experimental Studies of Epidermal Heat Flux Sensors for Measurements of Core Body Temperature. Advanced Healthcare Materials, 2016, 5, 119-127.	7.6	101
141	Flexible Electronics: Theoretical and Experimental Studies of Epidermal Heat Flux Sensors for Measurements of Core Body Temperature (Adv. Healthcare Mater. 1/2016). Advanced Healthcare Materials, 2016, 5, 2-2.	7.6	6
142	Water-Floating Giant Nanosheets from Helical Peptide Pentamers. ACS Nano, 2016, 10, 8263-8270.	14.6	40
143	Material science lesson from the biological photosystem. Nano Convergence, 2016, 3, 19.	12.1	18
144	Growth Mechanism of Strain-Dependent Morphological Change in PEDOT:PSS Films. Scientific Reports, 2016, 6, 25332.	3.3	33

#	Article	IF	CITATIONS
145	Highly Stretchable and Notch-Insensitive Hydrogel Based on Polyacrylamide and Milk Protein. ACS Applied Materials & Interfaces, 2016, 8, 29220-29226.	8.0	81
146	Graphene Quantum Sheet Catalyzed Silicon Photocathode for Selective CO ₂ Conversion to CO. Advanced Functional Materials, 2016, 26, 233-242.	14.9	77
147	Organolead Halide Perovskites for Low Operating Voltage Multilevel Resistive Switching. Advanced Materials, 2016, 28, 6562-6567.	21.0	285
148	Wafer-scale transferable molybdenum disulfide thin-film catalysts for photoelectrochemical hydrogen production. Energy and Environmental Science, 2016, 9, 2240-2248.	30.8	174
149	In Vitro and In Vivo Evaluation of Whitlockite Biocompatibility: Comparative Study with Hydroxyapatite and <i>î²</i> â€Tricalcium Phosphate. Advanced Healthcare Materials, 2016, 5, 128-136.	7.6	103
150	Spontaneously polarized lithium-doped zinc oxide nanowires as photoanodes for electrical water splitting. Journal of Materials Chemistry A, 2016, 4, 3223-3227.	10.3	14
151	Partially Oxidized Sub-10 nm MnO Nanocrystals with High Activity for Water Oxidation Catalysis. Scientific Reports, 2015, 5, 10279.	3.3	99
152	Phase transformation from hydroxyapatite to the secondary bone mineral, whitlockite. Journal of Materials Chemistry B, 2015, 3, 1342-1349.	5.8	66
153	N-doped graphene quantum sheets on silicon nanowire photocathodes for hydrogen production. Energy and Environmental Science, 2015, 8, 1329-1338.	30.8	136
154	Mn ₅ O ₈ Nanoparticles as Efficient Water Oxidation Catalysts at Neutral pH. ACS Catalysis, 2015, 5, 4624-4628.	11.2	123
155	Nano-hydroxyapatite modulates osteoblast lineage commitment by stimulation of DNA methylation and regulation of gene expression. Biomaterials, 2015, 65, 32-42.	11.4	106
156	Concave Rhombic Dodecahedral Au Nanocatalyst with Multiple High-Index Facets for CO ₂ Reduction. ACS Nano, 2015, 9, 8384-8393.	14.6	242
157	Hybrid Zâ€Scheme Using Photosystem I and BiVO ₄ for Hydrogen Production. Advanced Functional Materials, 2015, 25, 2369-2377.	14.9	65
158	Biofunctionalized Ceramic with Self-Assembled Networks of Nanochannels. ACS Nano, 2015, 9, 4447-4457.	14.6	15
159	Epidermal devices for noninvasive, precise, and continuous mapping of macrovascular and microvascular blood flow. Science Advances, 2015, 1, e1500701.	10.3	189
160	Coordination tuning of cobalt phosphates towards efficient water oxidation catalyst. Nature Communications, 2015, 6, 8253.	12.8	352
161	A tyrosine-rich peptide induced flower-like palladium nanostructure and its catalytic activity. RSC Advances, 2015, 5, 78026-78029.	3.6	9
162	Thermal Transport Characteristics of Human Skin Measured In Vivo Using Ultrathin Conformal Arrays of Thermal Sensors and Actuators. PLoS ONE, 2015, 10, e0118131.	2.5	70

#	Article	IF	CITATIONS
163	Self-assembled magnetic nanospheres with three-dimensional magnetic vortex. Applied Physics Letters, 2014, 105, .	3.3	22
164	Virus Templated Gold Nanocube Chain for SERS Nanoprobe. Small, 2014, 10, 3007-3011.	10.0	43
165	Tyrosine-mediated two-dimensional peptide assembly and its role as a bio-inspired catalytic scaffold. Nature Communications, 2014, 5, 3665.	12.8	98
166	One‣tep Synthesis of Nâ€doped Graphene Quantum Sheets from Monolayer Graphene by Nitrogen Plasma. Advanced Materials, 2014, 26, 3501-3505.	21.0	109
167	An iron oxide photoanode with hierarchical nanostructure for efficient water oxidation. Journal of Materials Chemistry A, 2014, 2, 2297-2305.	10.3	72
168	Revisiting Whitlockite, the Second Most Abundant Biomineral in Bone: Nanocrystal Synthesis in Physiologically Relevant Conditions and Biocompatibility Evaluation. ACS Nano, 2014, 8, 634-641.	14.6	151
169	A ferroelectric photocatalyst for enhancing hydrogen evolution: polarized particulate suspension. Physical Chemistry Chemical Physics, 2014, 16, 10408-10413.	2.8	95
170	Hydrated Manganese(II) Phosphate (Mn ₃ (PO ₄) ₂ ·3H ₂ O) as a Water Oxidation Catalyst. Journal of the American Chemical Society, 2014, 136, 7435-7443.	13.7	324
171	Hybrid system of semiconductor and photosynthetic protein. Nanotechnology, 2014, 25, 342001.	2.6	48
172	Full-Field Subwavelength Imaging Using a Scattering Superlens. Physical Review Letters, 2014, 113, 113901.	7.8	81
173	A New Water Oxidation Catalyst: Lithium Manganese Pyrophosphate with Tunable Mn Valency. Journal of the American Chemical Society, 2014, 136, 4201-4211.	13.7	136
174	Angle-resolved light scattering of individual rod-shaped bacteria based on Fourier transform light scattering. Scientific Reports, 2014, 4, 5090.	3.3	45
175	Extended gold nano-morphology diagram: synthesis of rhombic dodecahedra using CTAB and ascorbic acid. Journal of Materials Chemistry C, 2013, 1, 6861.	5.5	65
176	Enhanced conductivity of solution-processed indium tin oxide nanoparticle films by oxygen partial pressure controlled annealing. Journal of Materials Chemistry C, 2013, 1, 5953.	5.5	21
177	N-doped monolayer graphene catalyst on silicon photocathode for hydrogen production. Energy and Environmental Science, 2013, 6, 3658.	30.8	134
178	A new hematite photoanode doping strategy for solar water splitting: oxygen vacancy generation. Physical Chemistry Chemical Physics, 2013, 15, 2117.	2.8	126
179	Stretchingâ€Induced Growth of PEDOTâ€Rich Cores: A New Mechanism for Strainâ€Dependent Resistivity Change in PEDOT:PSS Films. Advanced Functional Materials, 2013, 23, 4020-4027.	14.9	54
180	Subwavelength light focusing using random nanoparticles. Nature Photonics, 2013, 7, 454-458.	31.4	160

#	Article	IF	CITATIONS
181	Protein/peptide based nanomaterials for energy application. Current Opinion in Biotechnology, 2013, 24, 599-605.	6.6	33
182	Self-Assembly of "S-Bilayersâ€; a Step Toward Expanding the Dimensionality of S-Layer Assemblies. ACS Nano, 2013, 7, 4946-4953.	14.6	16
183	Redox Cofactor from Biological Energy Transduction as Molecularly Tunable Energyâ€Storage Compound. Angewandte Chemie - International Edition, 2013, 52, 8322-8328.	13.8	147
184	Nanostructural dependence of hydrogen production in silicon photocathodes. Journal of Materials Chemistry A, 2013, 1, 5414.	10.3	55
185	Titelbild: Redox Cofactor from Biological Energy Transduction as Molecularly Tunable Energy-Storage Compound (Angew. Chem. 32/2013). Angewandte Chemie, 2013, 125, 8329-8329.	2.0	1
186	Subwavelength Light Control via Wavefront Shaping in Complex Media. , 2013, , .		0
187	Subwavelength Light Control via Wavefront Shaping in Complex Media. , 2013, , .		0
188	Multidimensional Assembly of S-Layer Proteins on Mobility-Controlled Polyelectrolyte Multilayers. ACS Macro Letters, 2012, 1, 1254-1257.	4.8	3
189	Enhanced performance of NaTaO3 using molecular co-catalyst [Mo3S4]4+ for water splitting into H2 and O2. Chemical Communications, 2012, 48, 10452.	4.1	44
190	Fatigueâ€Free, Electrically Reliable Copper Electrode with Nanohole Array. Small, 2012, 8, 3300-3306.	10.0	48
191	BMHP1-Derived Self-Assembling Peptides: Hierarchically Assembled Structures with Self-Healing Propensity and Potential for Tissue Engineering Applications. ACS Nano, 2011, 5, 1845-1859.	14.6	90
192	Clay nanoplate-chitosan hybrid hydrogels through electrostatic interaction. , 2011, , .		0
193	Electric-Field-Assisted Layer-by-Layer Assembly of Weakly Charged Polyelectrolyte Multilayers. Macromolecules, 2011, 44, 2866-2872.	4.8	42
194	Invited paper: Application of chitin and Chitosan toward electrochemical hybrid device. Electronic Materials Letters, 2011, 7, 13-16.	2.2	7
195	Folding of a singleâ€chain, informationâ€rich polypeptoid sequence into a highly ordered nanosheet. Biopolymers, 2011, 96, 586-595.	2.4	89
196	Free-floating ultrathin two-dimensional crystals from sequence-specific peptoid polymers. Nature Materials, 2010, 9, 454-460.	27.5	384
197	Synthesis and Microcontact Printing of Dual Endâ€Functionalized Mucinâ€like Glycopolymers for Microarray Applications. Angewandte Chemie - International Edition, 2009, 48, 4973-4976.	13.8	132
198	Peptide-Mediated Reduction of Silver Ions on Engineered Biological Scaffolds. ACS Nano, 2008, 2, 1480-1486.	14.6	139

#	Article	IF	CITATIONS
199	Stamped microbattery electrodes based on self-assembled M13 viruses. Proceedings of the National Academy of Sciences of the United States of America, 2008, 105, 17227-17231.	7.1	144
200	Controlling Surface Mobility in Interdiffusing Polyelectrolyte Multilayers. ACS Nano, 2008, 2, 561-571.	14.6	78
201	Solvent-Assisted Patterning of Polyelectrolyte Multilayers and Selective Deposition of Virus Assemblies. Nano Letters, 2008, 8, 1081-1089.	9.1	66
202	Spontaneous assembly of viruses on multilayered polymer surfaces. Nature Materials, 2006, 5, 234-240.	27.5	308
203	Virus-Enabled Synthesis and Assembly of Nanowires for Lithium Ion Battery Electrodes. Science, 2006, 312, 885-888.	12.6	1,756
204	Genetically Driven Assembly of Nanorings Based on the M13 Virus. Nano Letters, 2004, 4, 23-27.	9.1	108
205	Layer-by-Layer Surface Modification and Patterned Electrostatic Deposition of Quantum Dots. Nano Letters, 2004, 4, 1421-1425.	9.1	123
206	Multilayer diffusion barrier for copper metallization using a thin interlayer metal (M=Ru, Cr, and Zr) between two TiN films. Journal of Vacuum Science & Technology an Official Journal of the American Vacuum Society B, Microelectronics Processing and Phenomena, 2003, 21, 804.	1.6	22
207	Optimization of Al interlayer thickness for the multilayer diffusion barrier scheme in Cu metallization. Journal of Applied Physics, 2002, 92, 1099-1105.	2.5	19
208	Failure mechanism of a multilayer (TiN/Al/TiN) diffusion barrier between copper and silicon. Journal of Applied Physics, 2002, 92, 5512-5519.	2.5	17
209	Improved diffusion barrier by stuffing the grain boundaries of TiN with a thin Al interlayer for Cu metallization. Applied Physics Letters, 2001, 79, 2549-2551.	3.3	42